



CELL INJURY, REPAIR, AGING, AND APOPTOSIS

# Impaired Mitochondria Promote Aging-Associated Sebaceous Gland Dysfunction and Pathology



Noha S. Ahmed,<sup>\*†</sup> Jeremy B. Foote,<sup>‡§</sup> and Keshav K. Singh<sup>\*¶||</sup>

From the Departments of Genetics,<sup>\*</sup> Microbiology,<sup>‡</sup> Pathology,<sup>¶</sup> and Dermatology,<sup>||</sup> and the Animal Resources Program,<sup>§</sup> Heersink School of Medicine, The University of Alabama at Birmingham, Birmingham, Alabama; and the Department of Dermatology,<sup>†</sup> Zagazig University, Zagazig, Egypt

Accepted for publication  
July 14, 2022.

Address correspondence to  
Keshav K. Singh, Ph.D., De-  
partments of Genetics, Pathol-  
ogy, and Dermatology,  
Heersink School of Medicine,  
The University of Alabama at  
Birmingham, Kaul Genetics  
Bldg., Room 620, 720 I 20th St.  
S., Birmingham, AL 35294.  
E-mail: [kksingh@uab.edu](mailto:kksingh@uab.edu).

Mitochondrial dysfunction is one of the hallmarks of aging. Changes in sebaceous gland (SG) function and sebum production have been reported during aging. This study shows the direct effects of mitochondrial dysfunction on SG morphology and function. A mitochondrial DNA (mtDNA) deleter mouse was used as a model for introducing mitochondrial dysfunction in the whole animal. The effects on skin SGs and modified SGs of the eyelid, lip, clitoral, and preputial glands were characterized. The mtDNA deleter mice showed gross morphologic and histopathologic changes in SGs associated with increased infiltration by mast cells, neutrophils, and polarized macrophages. Consistently, there was increased expression of proinflammatory cytokines. The inflammatory changes were associated with abnormal sebocyte accumulation of lipid, defective sebum delivery at the skin surface, and the up-regulation of key lipogenesis-regulating genes and androgen receptor. The mtDNA deleter mice expressed aging-associated senescent marker. Increased sebocyte proliferation and aberrant expression of stem cell markers were observed. These studies provide, for the first time, a causal link between mitochondrial dysfunction and abnormal sebocyte function within sebaceous and modified SGs throughout the whole body of the animal. They suggest that mtDNA deleter mouse may serve as a novel tool to develop targeted therapeutics to address SG disorders in aging humans. (*Am J Pathol* 2022, 192: 1546–1558; <https://doi.org/10.1016/j.ajpath.2022.07.006>)

Sebaceous glands (SGs) are exocrine glands with holocrine secretion, which means the whole cell constitutes a secretory product on cell membrane disruption.<sup>1,2</sup> Sebaceous glands are located mainly in the dermis, arise as an outgrowth of the outer root sheath of the hair follicle, and remain attached to the hair follicle throughout adult life. They secrete lipid-rich sebum into the hair canal that passes up to the skin surface and plays a crucial role in skin and hair moisturization, barrier acquisition, water evaporation from the skin surface, and hair growth.<sup>1,3</sup> Sebum is rich in antioxidants, antimicrobial lipids, and pheromones.<sup>3–6</sup> Besides the hair follicle-associated SG, other types of modified SGs (MSGs; termed ectopic glands) are found at mucosal sites, including oral epithelium, perianal region, eyelids SGs (meibomian glands),<sup>7,8</sup> the preputial gland in males, and clitoral gland in females.<sup>9</sup> The primary SG and MSG cell type is the sebocyte with peripheral flattened

undifferentiated mitotically active sebocytes that proceed centrally to mature fully differentiated sebocytes.<sup>6</sup> There is a continuous balance between sebaceous gland proliferation and differentiation throughout adult life.<sup>10</sup> Sebaceous gland activity is strongly influenced by steroid and peptide hormones,<sup>11</sup> especially androgen, which is known to stimulate sebocyte proliferation<sup>12</sup> and lipid production.<sup>12,13</sup> In addition, neuroendocrine regulators (substance-P, corticotropin-releasing hormone, and proopiomelanocortin-derived peptides) and insulin-like growth factor-1 play important roles in the control of SG activity.<sup>3,14,15</sup> Lastly, peroxisome proliferator-activated receptors (PPARs) play important

Supported in part by NIH R21OD031970 and Yuva Biosciences (research in the laboratory of K.K.S.).

Disclosures: K.K.S. is the scientific founder and chief scientific advisor at Yuva Biosciences. N.S.A. and J.B.F. declare no conflicts of interest.

role(s) controlling sebocyte proliferation and lipogenesis.<sup>16–18</sup> Sebaceous gland disorders are of particular interest as they are involved in the pathogenesis of diverse diseases associated with human aging that involve morphologic changes and alteration of sebaceous gland activity or changes in sebum composition.<sup>19</sup> Mitochondrial dysfunction contributes to skin aging.<sup>20,21</sup> Sebaceous glands, described as the brain of the skin, are active and demand high energy consumption.<sup>22</sup> A wide spectrum of modifications in mitochondria and its DNA occurs during aging, ranging from disorganized mitochondrial structure and impaired oxidative phosphorylation to increased mitochondrial production of reactive oxygen species that results in increased oxidative damage to DNA, proteins, and lipids along with the accumulation of mutation or depletion of mitochondrial DNA (mtDNA).<sup>23</sup> To our knowledge, no previous study has described a direct causal link between aging-associated mitochondrial dysfunction and sebaceous gland function at different body sites. Utilizing the mtDNA depleter mouse<sup>24</sup> enabled us to determine the role of mitochondria in sebaceous gland homeostasis in the whole animal.

## Materials and Methods

### Animal and Experimental Design

We used in this study a mouse model with whole-body mtDNA depletion, where the dominant-negative polymerase gamma (POLG) is ubiquitously expressed in the presence of doxycycline (200 mg/kg in diet), leading to depletion of mtDNA.<sup>24</sup> We started the doxycycline diet at the age of 8 weeks and assigned the mice to two groups with three mice in each group: control [POLG positive/reverse tetracycline-controlled transactivator (rtTA) negative] and mtDNA depleter groups (POLG positive/rtTA positive) with males and females in each group; we followed up the mice weekly after doxycycline induction. Digital images were collected weekly using a digital camera (DSC HX40; Sony, San Diego, CA). All animal experiments were performed following protocols approved by the Laboratory Animal Care and Use Committee of the University of Alabama at Birmingham.

### Histology and Immunohistochemistry

Mice tissues were collected at each time point for paraffin sections; tissues were fixed in 10% neutral-buffered formalin, embedded in paraffin, sectioned at 5  $\mu$ m, deparaffinized, and stained with hematoxylin and eosin for histology and modified Giemsa stain (Sigma, St. Louis, MO; GS500) to detect mast cells. Immunohistochemistry was performed using specific antibodies: CD163 (catalog number Ab182422; rabbit; 1:200), myeloperoxidase (catalog number Ab208670; rabbit; 1:200), Ki-67 (catalog number Ab16667; rabbit; 1:200), SRY-box transcription factor 9 (Sox9) (catalog number Ab185230; rabbit; 1:500), leucine-rich repeat-containing G-protein

coupled receptor 5 (Lgr5) (catalog number Ab75732; rabbit; 1:100), and Lgr6 (catalog number Ab126747; rabbit; 1:100). Briefly, tissue sections were deparaffinized and underwent antigen retrieval using antigen unmasking solution in double-distilled water (catalog number H-3301; Vector, Burlingame, CA); then, they were blocked with 10% normal goat serum and incubated overnight with specific antibodies. The signal was visualized by subsequent incubation with fluorescence-tagged appropriate secondary antibodies (Alexa 568-tagged; catalog number TI-1000-1.5;  $\alpha$ -rabbit; 1:200). Scanned images were obtained using a scanner microscope (BZ-X810; Keyence, Itasca, IL) and image snaps using a microscope (1X-S8F2; Olympus, Tokyo, Japan).

### Detection of Lipids

Mouse tissues were collected and embedded in mounting medium (Tissue-Tek O.C.T.; Sakura Finetek USA, Inc., Torrance, CA), snap frozen in liquid nitrogen, and stored at  $-80^{\circ}\text{C}$ . Next, sections (12  $\mu$ m thick) were obtained and attached to glass slides, air dried for 90 minutes at room temperature, and then stained with Oil Red O (ORO) dye to detect the presence of lipids. Briefly, sections were fixed in formalin and washed with running tap water for 3 minutes. Next, samples were rinsed with 60% isopropanol (Sigma; 59,301) and then stained for 15 minutes with freshly prepared ORO working solution (Sigma; O9755). Samples were then briefly rinsed in 60% isopropanol, washed thoroughly in water, counterstained with Mayer hematoxylin solution, and mounted with aqueous mounting media (nine parts of glycerol and one part phosphate-buffered saline).<sup>25</sup> Image snaps have been taken using a microscope (Olympus 1X-S8F2) and quantified using the ImageJ software desktop version 1.53q (NIH, Bethesda, MD; <http://imagej.nih.gov/ij>, last accessed January 14, 2022).

### Aging-Associated Senescence Marker

Detection of lipofuscin senescence-associated marker was done using Sudan black B (J62268; Alfa Aesar, Tewksbury, MA); for staining, formalin-fixed paraffin sections were dewaxed, hydrated gradually until 70% ethanol, and covered with a drop of freshly prepared Sudan black B solution for 8 minutes; then, the sections were rapidly immersed in 50% ethanol for a few minutes, washed with double-distilled water, and then mounted with 40% glycerol/tris-buffered saline.<sup>26</sup> Image snaps have been taken using a microscope (Olympus 1X-S8F2) and quantified using the ImageJ software desktop version 1.53q.

### Real-Time PCR

Total RNA was isolated from each tissue using TRIzol (Invitrogen, Carlsbad, CA), and 500 to 1000 ng RNA was used to prepare cDNA using the Iscript cDNA synthesis kit (Bio-Rad Laboratories, Hercules, CA). cDNA was used to

**Table 1** List of Primers Used in the Study

Target	Forward primer	Reverse primer
RT-PCR		
<i>POLG1</i>	5'-CAAGGTCCAGAGAGAAACTG-3'	5'-CTCTGTACCACCCAATTCAC-3'
<i>CAG-rtTA</i>	5'-CTGCTGTCCATTTCCTTATTC-3'	5'-CGAAACTCTGGTTGACATG-3'
RT-qPCR		
<i>COX2</i>	5'-ACACACTCTATCACTGGCACC-3'	5'-TTCAGGGGAGAAGCGTTTGC-3'
<i>Tnf</i>	5'-GCCTCTTCTCATTCCTGCTTG-3'	5'-CTGATGAGAGGGAGGCCATT-3'
<i>Il1r-1</i>	5'-GCACGCCAGGAGAATATGA-3'	5'-AGAGGACACTTGC GAATATCAA-3'
<i>Il-6</i>	5'-ATCCAGTTGCCCTTCTTGGGACT-3'	5'-TAAGCCTCCGACTTGTGAAGTGGT-3'
<i>Sox9</i>	5'-AGGAAGCTGGCAGACCAGTA-3'	5'-CTCCTCCACGAAGGGTCTCT-3'
<i>Lgr5</i>	5'-CAGCGTCTTCACCTCTACC-3'	5'-TGTGTCAAAGCATTTCCA GC-3'
<i>Lgr6</i>	5'-CCGGGACCAGGAGGTGAG-3'	5'-CACAGCGCAAAGCCACAG-3'
<i>Gli1</i>	5'-GAGGTTGGGATGAAGAAGCA-3'	5'-CTTGTGGTGGAGTCATTGGA-3'
<i>Gli2</i>	5'-CGAGTGCAACGTTTCCACAG-3'	5'-GTCAGGTTGCTGTCTACGCT-3'
<i>Ppara</i>	5'-AGTTCGGGAACAAGACGTTG-3'	5'-CAGTGGGGAGAGAGGACAGA-3'
<i>Pparg</i>	5'-TGCACTGCCTATGAGCACTT-3'	5'-GAATGCGAGTGGTCTTCCAT-3'
<i>Ppard</i>	5'-AGATGAAGACAAACCCACGG-3'	5'-CTGTGGCTGTTCCATGACTG-3'
<i>Scd1</i>	5'-TGGAGACGGGAGTCACAAGA-3'	5'-ACACCCCGATAGCAATATCCAG-3'
<i>Prdm1</i>	5'-ACCAAGGAACCTGCTTTTCA-3'	5'-TAGACTTCACCGATGAGGGG-3'
<i>Plin2</i>	5'-CCCGTATTTGAGATCCGTGT-3'	5'-TAGGTATTGGCAACCGCAAT-3'
<i>Ar</i>	5'-TATGTGCCAGCAGAAACGATTGTA-3'	5'-CGGTACTCATTGAAAACCAAGTCA-3'

RT-qPCR, quantitative RT-PCR.

measure relative gene expression by RT-PCR using a Green Taq PCR mixture (Promega, Madison, WI). PCR products were run on 1.5% agarose gel and imaged using the Odyssey FC gel documentation system (Lincoln, NE). For quantitative RT-PCR, amplification of cDNA was performed using a Luna Universal qPCR Master Mix (number M3003; NEB, Ipswich, MA) on a Roche LightCycler480 Real-Time PCR system (Rotkreuz, Switzerland). Three replicates were used in each PCR, and  $\beta$ -actin was used as an internal control. Primers used in this study are indicated in Table 1.

### Statistical Analysis

Statistical analyses were performed using unpaired *t*-test. Data are expressed as means  $\pm$  SD;  $P > 0.05$  was considered nonsignificant;  $*P \leq 0.05$ ,  $**P \leq 0.01$ ,  $***P \leq 0.001$ , and  $****P \leq 0.0001$  were considered significant.

## Results

### Mitochondrial Dysfunction Induces Abnormal Phenotypes at Sites of Sebaceous Glands

The mtDNA deleter mouse model was used, which shows the signs of aging in the form of hair loss and wrinkles.<sup>24</sup> Time-course images showed gross evidence of MSG dysfunction of eyelids (Figure 1A), lip (Figure 1D), prepuce (Figure 1E), and clitoris (Figure 1F) at 4, 6, and 8 months of doxycycline induction. Mitochondrial DNA depletion in mice after 8 months of doxycycline induction resulted in gross evidence of SG dysfunction, manifesting as skin xerosis, erythema, and pruritus (Figure 1Bi). Within these

regions, yellow umbilicated papules (Figure 1Bii), resembling SG hyperplasia seen in humans, and yellow macules that appear underneath stretched face skin (Figure 1Biii) were noted. On closer inspection, mtDNA deleter mice consistently developed skin erythema and scaling at seborrhic sites located behind ears (Figure 1Biv), inside the external ear canal (Figure 1Bv), on neck flexure accompanied with ulceration (Figure 1Bvi), and around eyes (Figure 1Bvii), consistent with clinical signs of seborrhic dermatitis in aging humans. Changes at sites of MSGs included swelling on the upper and lower eyelids, erythema, and telangiectasia with irregular lid margin (Figure 1Ci and ii) and swelling and redness in the lip region (Figure 1Ciii) and the clitoris (Figure 1Civ) in female mice, which on dissection revealed gross evidence of abscessation in some animals (Figure 1Cv). Similarly, male mice had swelling of prepuce externally (Figure 1Cvi) and enlargement of the preputial gland observed grossly and on dissection (Figure 1Cvii).

### Histopathologic Changes in Sebaceous Glands Associated with Mitochondrial Dysfunction

To confirm that the gross changes were associated with morphologic changes in the SGs and MSGs, haired skin was collected from the dorsal back region, eyelids, lip, and harderian, preputial, clitoral, and zymbal glands from mtDNA deleter and littermate control mice, at 8 months after doxycycline treatment. Hematoxylin and eosin staining revealed corresponding evidence of SG hyperplasia, as evidenced by increased glandular size, cellular and nuclear atypia, an increase in mitotic figures within SGs from the skin (Figure 2A) and MSGs of the eyelid meibomian gland

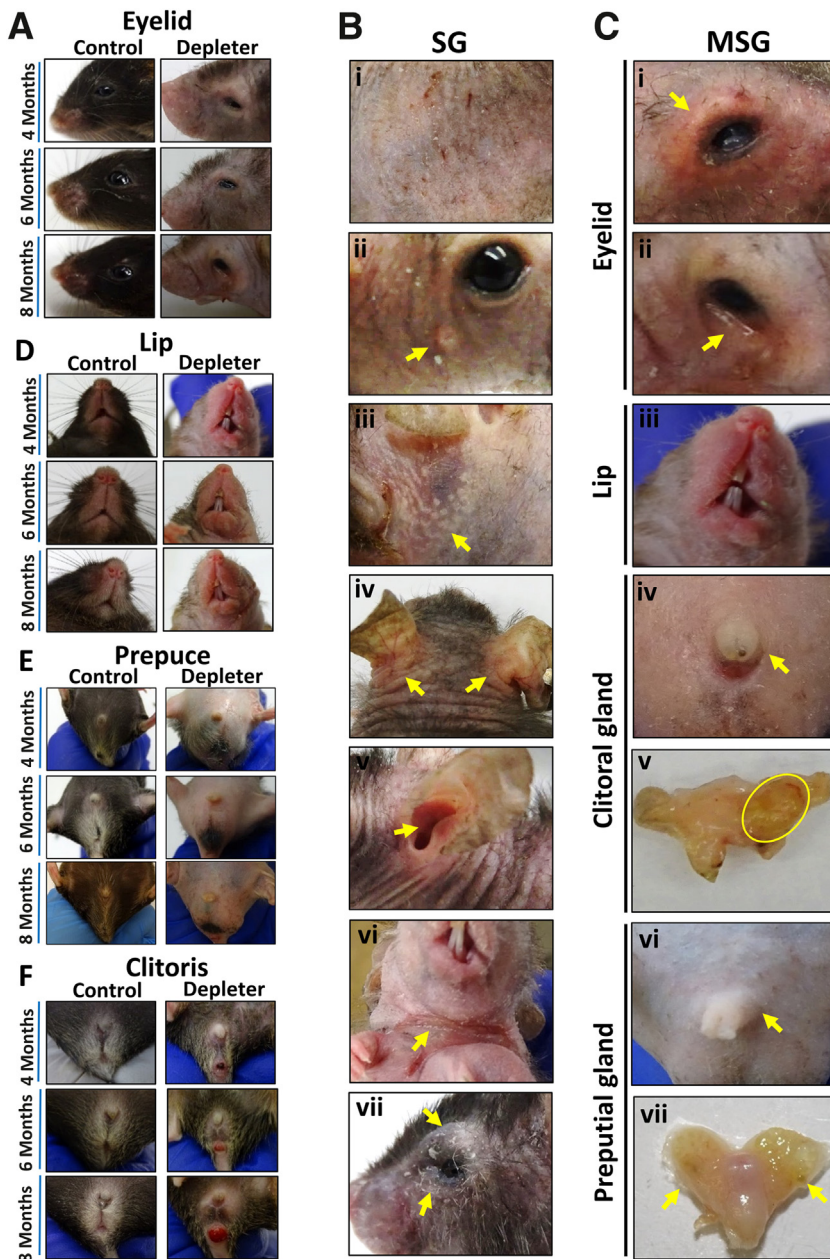


**Figure 1** Phenotypic sebaceous gland (SG) and modified sebaceous gland (MSG) abnormalities due to mitochondrial dysfunction. Representative images were taken of mitochondrial DNA (mtDNA) depleter mice after doxycycline diet induction showing. Representative time-course images of mice taken over 4, 6, and 8 months of doxycycline induction for control and mtDNA depleter mice. **A:** Eyelid images showing no changes in control mice over time, and mtDNA depleter mice showing loss of eyelashes with erythematous scaly irregular lid margins. **B:** The spectrum of cutaneous phenotypes suggestive of SG dysfunction observed in the mtDNA depleter mouse model, including the following: i) scaly erythematous skin, ii) yellow umbilicated papules (**yellow arrow**) on the face, iii) deposition of yellow plaques in stretched skin (**yellow arrow**), iv) erythema and scaling behind ears (**yellow arrows**) and v) inside the ear (**yellow arrow**), vi) erythematous neck flexure accompanied with ulceration (**yellow arrow**), and vii) swelling, erythema, and scaling on eyelid margins (**yellow arrows**). **C:** The spectrum of phenotypes suggestive of MSG dysfunction observed in the mtDNA depleter mouse model, comprising the following: i) swollen, erythematous eyelids with telangiectasia (**yellow arrow**), ii) erythematous and irregular lower lid margin (**yellow arrow**), iii) enlarged and erythematous upper and lower lips, iv) enlarged external clitoris (**yellow arrow**) that shows v) enlargement of clitoral glands on dissection and abscess formation (yellow oval) in female mice, and vi) enlargement of prepuce externally (**yellow arrow**) with vii) enlarged preputial glands on dissection in male mice (**yellow arrows**). **D:** Lip images show no differences in control mice over time, whereas mtDNA depleter mice show lip erythema and swelling. **E:** Swelling of the prepuce in male mtDNA depleter mice. **F:** Swelling of the clitoris in female mtDNA depleter mice.

(Figure 2B), lips (Figure 2C), harderian gland (Figure 2D), preputial gland (Figure 2E), clitoral gland (Figure 2F), and zymbal gland (Figure 2G) in mtDNA depleter mice in comparison to littermate controls. In addition, variable amounts of periglandular and intraglandular inflammation were noted around skin SGs (Figure 2A), MSGs (Figure 2, B–G), and meibomian, harderian, preputial, clitoral, and zymbal glands from mtDNA depleter, but not littermate control mice. Inflammatory infiltrate ranged in composition from pigmented macrophages, and lymphocytes, to large numbers of neutrophils and macrophages in particular within preputial and clitoral glands, where the typical glandular structure was effaced by pyogranulomatous inflammation (Figure 2, F and G). Furthermore, within

severely inflamed preputial and clitoral glands, free lipid material was noted in the glandular interstitia and surrounded by a pyogranulomatous inflammatory infiltrate and multinucleated giant cells (Figure 2, F and G) compared with typical structure and absent inflammation in littermate controls treated with doxycycline.

### Mitochondrial Dysfunction Causes Severe Inflammation of Sebaceous Glands

Chronic inflammation is a key feature of aging<sup>27–29</sup> that eventually leads to decreased organ function. Previous studies have demonstrated a significant role for mtDNA

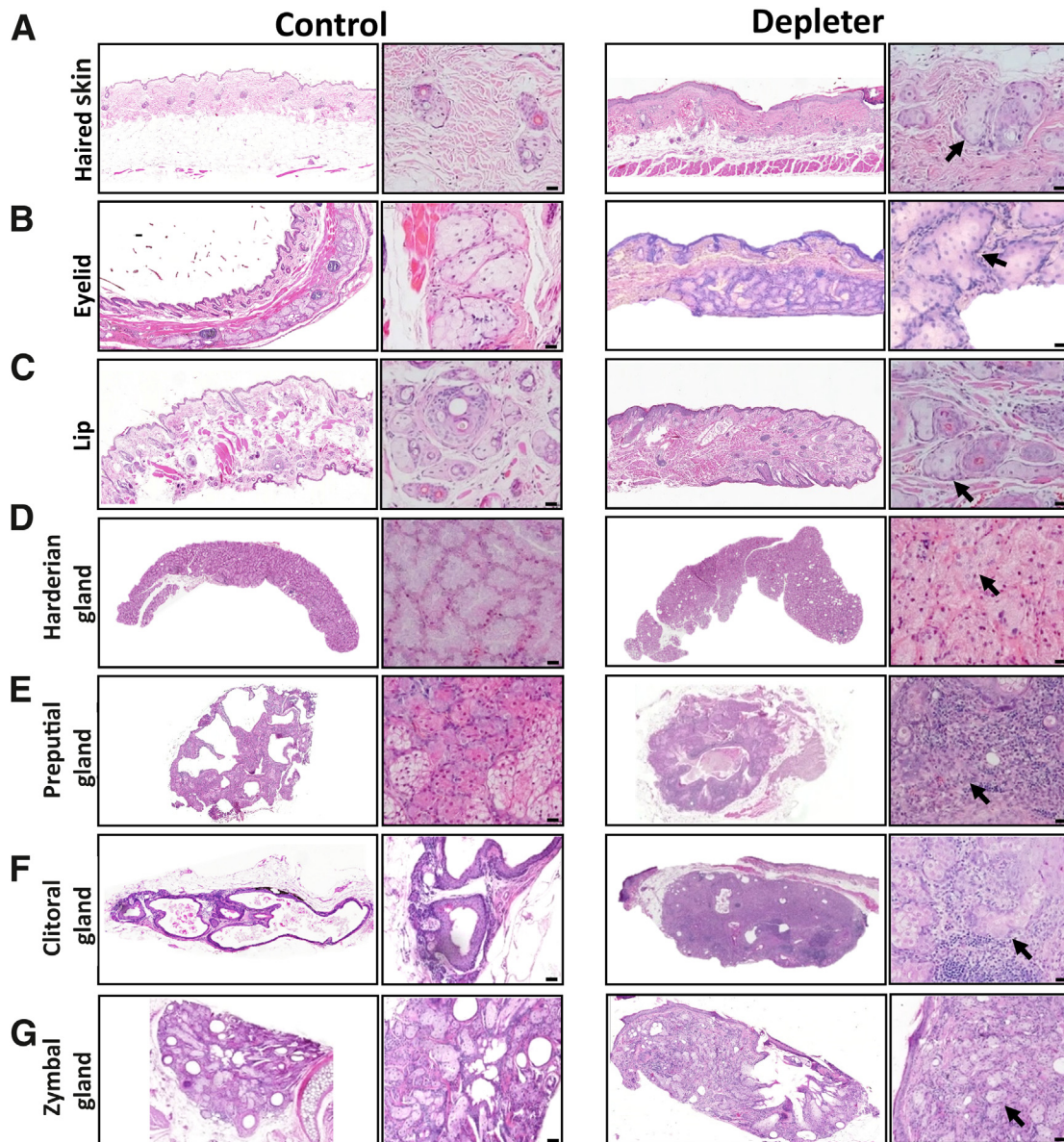
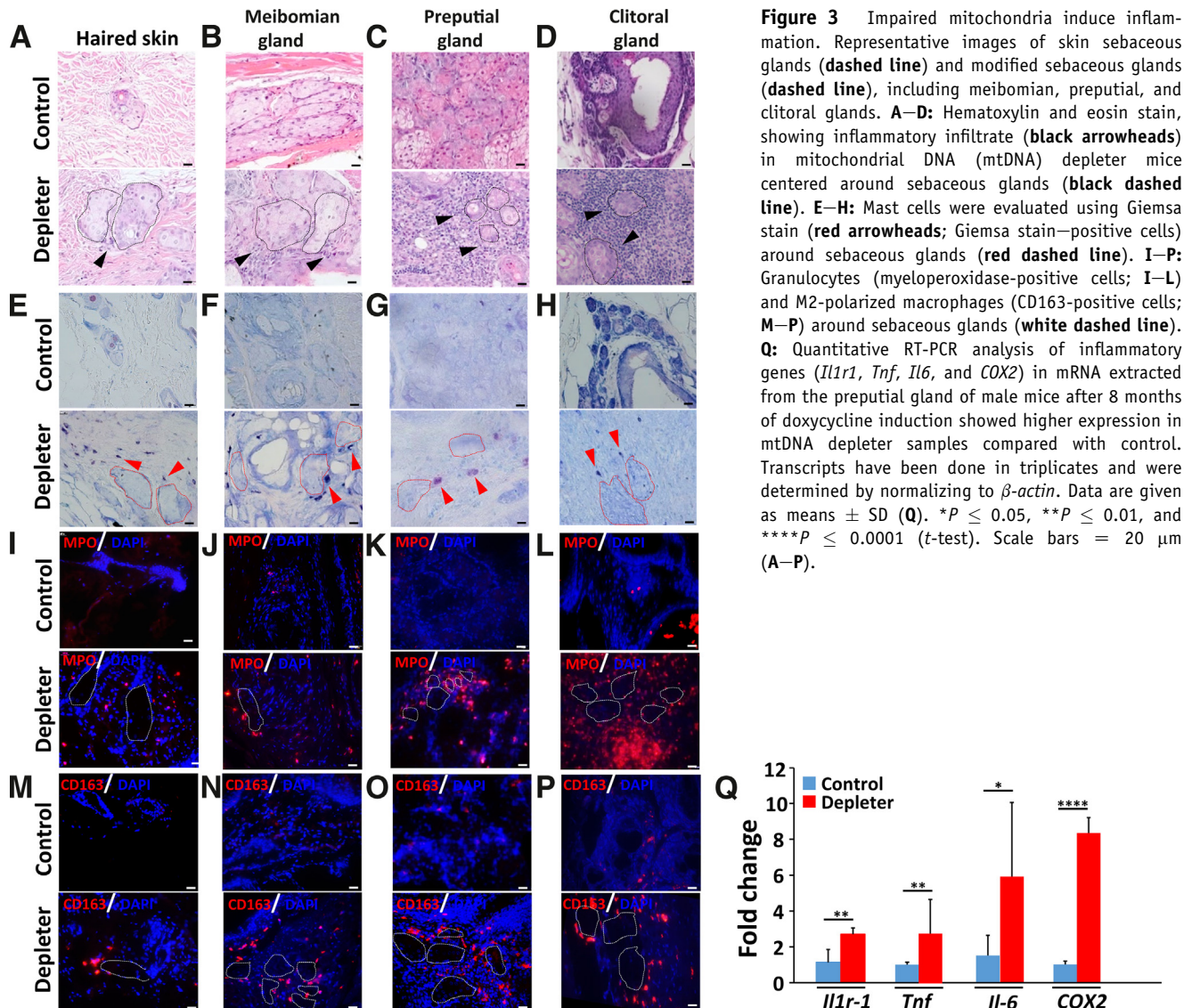


**Figure 2** Mitochondrial dysfunction–induced histopathologic alterations in sebaceous and modified sebaceous glands. **A:** Representative hematoxylin and eosin–stained sections after 8 months of doxycycline induction of skin-associated sebaceous glands. **B–G:** Modified sebaceous glands of eyelids (meibomian glands; **B**), lips (**C**), harderian gland (**D**), preputial gland (**E**), clitoral gland (**F**), and zymbal gland (**G**). Hyperplastic changes associated with sebocytes (**black arrows**) and variable amounts of mixed inflammatory infiltrate within the dermis/submucosa. Hyperplastic changes include increased cell and nuclear size, irregular cellular orientation within glands, and inflammation, most notably within clitoral and preputial glands. Scale bars = 50  $\mu$ m (**A–G**).

loss and age-associated inflammation within the skin of the mtDNA depletor model.<sup>24</sup> Herein, all collected tissues from the skin, eyelids, and preputial and clitoral glands shared a common observation of mixed inflammatory infiltrate surrounding SGs and MSGs, as detected with hematoxylin and eosin staining (**Figure 3, A–D**). More heavy infiltration was observed at sites of preputial and clitoral glands up to the formation of pyogranulomatous reaction that destroys the whole glandular architecture (**Figure 3, C and D**). To better characterize the types of inflammatory cells, tissue sections were stained with special (Giemsa) and immunohistochemical (myeloperoxidase

and CD163) stains. These were used to identify specific myeloid cell subsets noted to be involved in dermal inflammation in this model and to determine whether these inflammatory cells infiltrated SGs and MSGs. Giemsa staining revealed an increased number of mast cells with metachromatic granules around SGs and MSGs (**Figure 3, E–H**). Similar increases in periglandular myeloperoxidase-positive neutrophils (**Figure 3, I–L**) and CD163<sup>+</sup> M2 polarized macrophages (**Figure 3, M–P**) were noted in mtDNA depletor mice around SGs and MSGs. Sebocytes can also produce a wide range of proinflammatory cytokines and lipid-derived mediators.<sup>16,30</sup> To determine



whether sebocytes produced proinflammatory mediators, quantitative RT-PCR analysis of SG inflammatory expressed genes was performed in preputial glands of male mice. Significantly higher expression of *Il1r1* ( $P = 0.005$ ), *Tnf* ( $P = 0.009$ ), fourfold increase in *Il6* ( $P = 0.02$ ), and eightfold increase in *COX2* ( $P = 0.0001$ ) in mtDNA depletor samples was observed compared with control (**Figure 3Q**). Transcripts were used in triplicates and were determined by normalizing to  $\beta$ -actin.

#### Lipid Accumulation in Sebaceous Glands as a Result of Mitochondrial Dysfunction

Mitochondrial dysfunction has been reported to result in intracellular accumulation of lipid droplets in adipocytes.<sup>31</sup> ORO staining was used to determine abnormal lipid accumulation within SGs of mtDNA depletor mice. An increased abundance of large lipid droplets within the skin SGs as

compared to littermate controls was observed (**Figure 4A**). This was supported by significantly increased ORO integrated density in the skin SGs ( $P = 0.0005$ ) (**Figure 4B**) and meibomian glands (**Figure 4C**). Additionally, ORO integrated density was significantly increased in the meibomian glands ( $P = 0.001$ ) (**Figure 4D**) of mtDNA depletor mice compared with littermate controls. Grossly evident dilation of meibomian glands was noted in mtDNA depletor mice (**Figure 4G**) compared with littermate controls treated with doxycycline for 2 months. Within haired skin, mtDNA depletor mice had less skin surface lipid than littermate controls (**Figure 4E**), evidenced by significantly less ORO integrated density on the skin surface ( $P = 0.05$ ) (**Figure 4F**). Evaluation of lipogenesis-regulating genes in preputial gland (**Figure 4H**) indicated significant up-regulation of *Scd1* ( $P = 0.006$ ), *Prdm1* ( $P = 0.003$ ), *Plin2* ( $P = 0.01$ ), and *Pparg* ( $P = 0.000007$ ) and up-regulation of *Pparg* ( $P = 0.15$ ), with significant down-

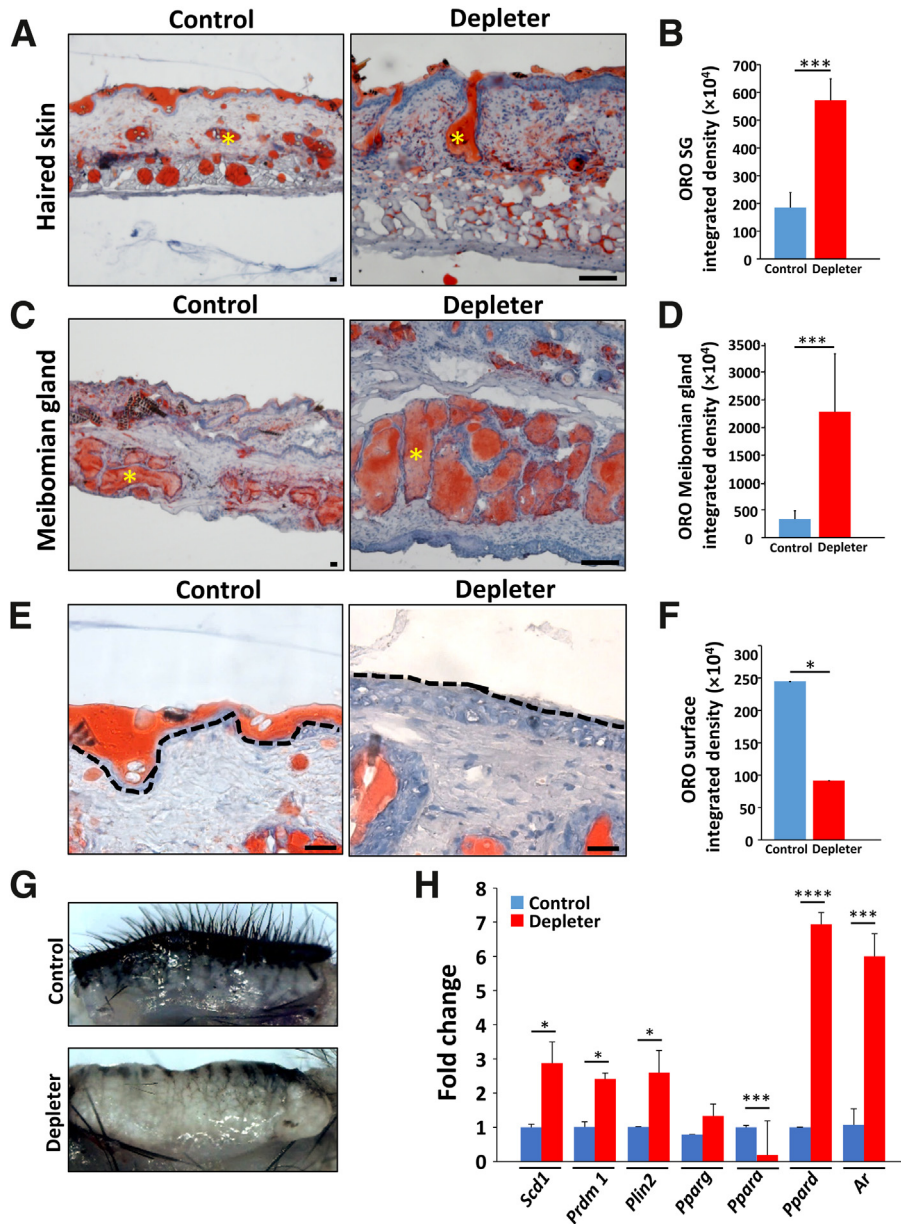


**Figure 4** Abnormal lipid accumulation in sebaceous glands (SGs) and modified sebaceous glands. Representative images of skin and eyelid stained with Oil Red O (ORO) for lipids, showing lipid accumulation in mitochondrial DNA (mtDNA) depletor mice after 8 months of doxycycline induction. **A:** Skin sebaceous glands (**yellow asterisks**). **B:** Quantification of ORO integrated density in SG compared with control littermate. **C:** Modified eyelid sebaceous glands (meibomian glands; **yellow asterisks**). **D:** Quantification of ORO integrated density in meibomian glands compared with control littermate. **E:** Oil Red O stain, showing no or minimal lipid layer on skin surface compared with continuous lipid layer in control skin (**black dashed line**). **F:** Quantification of ORO integrated density on the skin surface. **G:** Representative gross image, showing distension of meibomian glands in mtDNA depletor mice after 2 months of doxycycline induction compared with control. **H:** Quantitative RT-PCR analysis of lipogenesis-regulating genes (*Scd1*, *Prdm1*, *Plin2*, *Ppara*, *Pparg*, and *Ppard*) and androgen receptor gene (*Ar*) in mRNA extracted from the preputial gland of male mice after 8 months of doxycycline induction, showing higher expression in mtDNA depletor samples compared with control. Transcripts were done in triplicates and were determined by normalizing to  $\beta$ -actin. Data are given as means  $\pm$  SD (**B**, **D**, **F**, and **H**). \* $P \leq 0.05$ , \*\*\* $P \leq 0.001$ , and \*\*\*\* $P \leq 0.0001$  (*t*-test). Scale bars = 20  $\mu$ m (**A**, **C**, and **E**).

regulation of *Ppara* ( $P = 0.0007$ ) associated with significant up-regulation of androgen receptors (*Ar*;  $P = 0.0005$ ) in mtDNA depletor mice compared with littermate controls. These gross, histologic, and gene analysis findings indicate that oxidative inflammation in mtDNA depletor mice affects the production and localization of sebaceous gland lipid secretions.

### Mitochondrial Dysfunction Induces Accumulation of Age-Associated Senescent Markers

To determine whether mitochondrial dysfunction induces senescence, we evaluated lipofuscin, a marker of age-associated senescence,<sup>32</sup> and a marker of oxidation of lipoproteins within lysosomes. Significant increases in

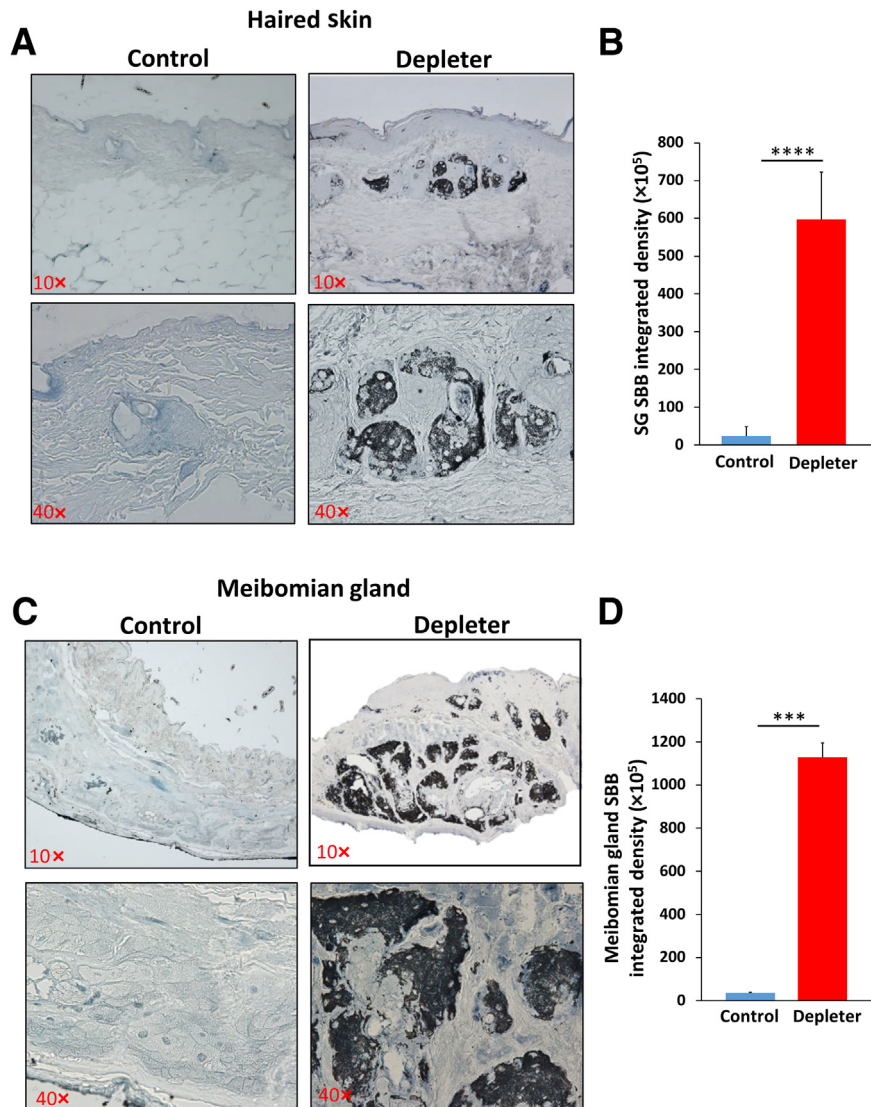


**Figure 5** Mitochondrial dysfunction causes accumulation of senescent cells in sebaceous glands (SGs). Representative images stained with Sudan black B (SBB) for lipofuscin detection in skin sebaceous glands (A) and eyelid meibomian glands (C), showing characteristic deposition of blue-black pigments that represent positivity for lipofuscin in sebaceous glands of mitochondrial DNA deleter mice compared with control. Quantification of SBB integrated density in skin SG (B) and meibomian glands (D). Data are given as means  $\pm$  SD (B and D).  $***P \leq 0.001$ ,  $****P \leq 0.0001$  (*t*-test). Original magnification,  $\times 10$  (A and C, top panels);  $\times 40$  (A and C, bottom panels).

cytoplasmic expression of lipofuscin within sebocytes in skin SGs were observed (Figure 5A). This was accompanied by significantly increased Sudan black B integrated density (Figure 5B) ( $P = 0.0001$ ), and in meibomian glands (Figure 5C), as evidenced by considerably increased Sudan black B integrated density (Figure 5D) ( $P = 0.0002$ ), of mtDNA deleter mice but not littermate controls.

#### Mitochondrial Dysfunction Promotes Changes in Expression of Stem Cell Markers

The maintenance of SGs depends on different progenitor cells at the periphery of the gland,<sup>33–35</sup> where there is a balance between proliferation and differentiation.<sup>10</sup> Immunohistochemical staining with proliferative marker Ki-67

showed a significant increase in cellular proliferation (Figure 6G) ( $P = 0.006$ ) at the periphery of skin SGs (Figure 6A), meibomian glands (Figure 6B), and preputial gland (Figure 6C), detected by positive Ki-67 staining.

Aging is associated with a decline in stem cell function and tissue regenerative capacity<sup>36–38</sup> that has been previously reported to result from mitochondrial dysfunction.<sup>39,40</sup> mRNA and protein expression of stem cell-associated markers was evaluated, beginning with Sox9. Its over-expression has enhanced sebocyte proliferation, differentiation, and lipogenesis.<sup>41</sup> Interestingly, mtDNA deleter mice showed significant up-regulation of nuclear Sox9 protein expression within skin SGs (Figure 6D), meibomian glands (Figure 6E), and preputial glands (Figure 6F). Quantitative RT-PCR was used to confirm the changes in



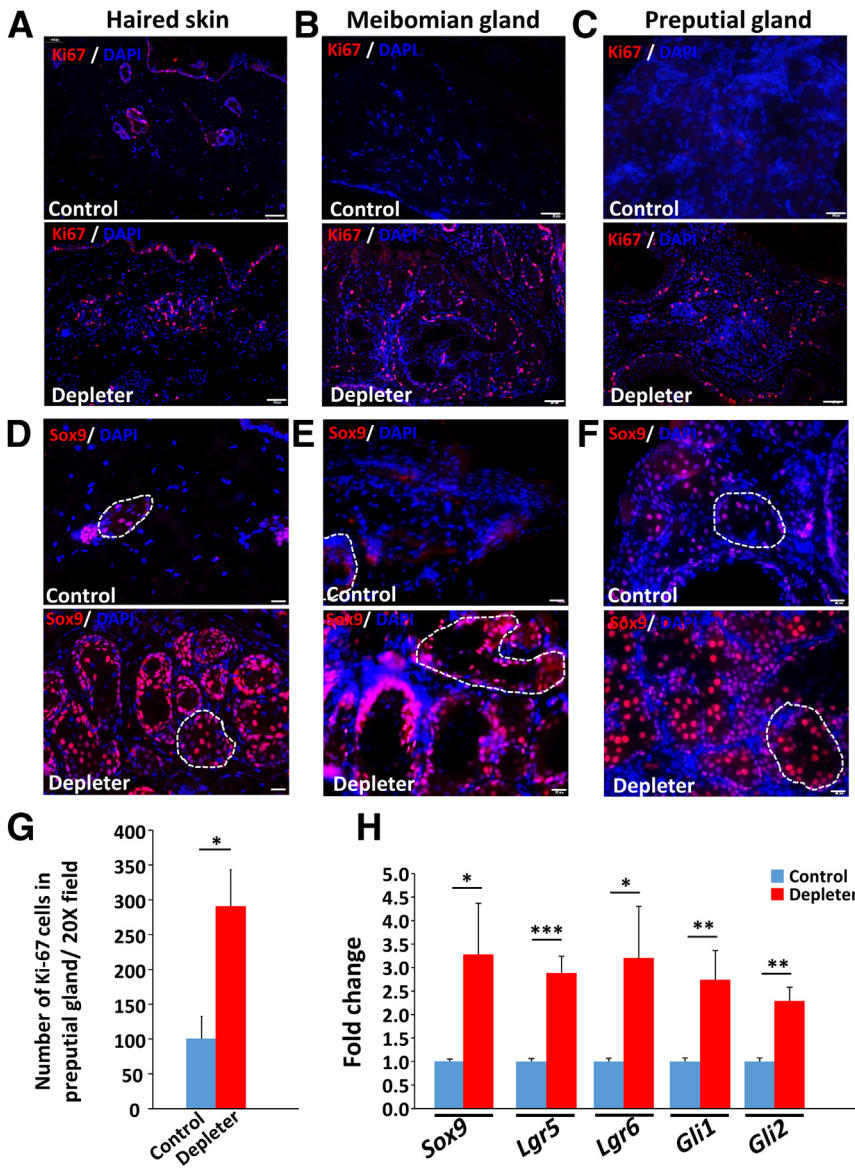


**Figure 6** Abnormal proliferation and changes in expression of stem cell markers. **A–C:** Representative immunofluorescence staining of skin sebaceous glands and modified sebaceous glands (**A**), eyelid meibomian glands (**B**), and preputial gland (**C**) with proliferation marker Ki-67 (red) counterstained with nuclear stain DAPI (blue), showing higher expression in sebaceous glands of mitochondrial DNA (mtDNA) depletor mice compared with control. **D–F:** Immunohistochemical staining of skin (**D**), eyelid meibomian glands (**E**), and preputial gland (**F**) sections with Sox9 (red) with nuclei counterstained with DAPI (blue) in mtDNA depletor mice compared with control. Sebaceous gland marked with the **white dashed line**. **G:** Quantitative analysis of Ki-67–stained cells in the preputial gland. **H:** Quantitative RT-PCR analysis of sebaceous gland stem cell expressed genes (*Sox9*, *Lgr6*, *Lgr5*, *Gli1*, and *Gli2*) in the preputial gland of mtDNA depletor mice compared with control. Transcripts were done in triplicates and were determined by normalizing to  $\beta$ -actin. Data are given as means  $\pm$  SD (**G** and **H**). \* $P \leq 0.05$ , \*\* $P \leq 0.01$ , and \*\*\* $P \leq 0.001$  (*t*-test). Scale bars: 50  $\mu$ m (**A–C**); 20  $\mu$ m (**D–F**).

gene expression of stem cell markers (Figure 6H). Higher expression of *Sox9* ( $P = 0.02$ ) was seen. The study evaluated the expression of *Lgr6*, which is a marker of long-lived, quiescent stem cells<sup>42–45</sup> and has been reported to contribute to SG regeneration.<sup>46</sup> mtDNA depletor mice had significantly higher expression of *Lgr6* ( $P = 0.03$ ), *Lgr5* ( $P = 0.001$ ), *Gli1* ( $P = 0.009$ ), and *Gli2* ( $P = 0.002$ ) in preputial gland. These findings confirm the expression of the stem cell markers *Lgr6* and *Lgr5*, and notch ligands *Gli1* and *Gli2* within sebocytes. Together, these studies suggest mitochondrial dysfunction causes aberrant expression of stem cell markers in sebocytes.

**Discussion**

Mitochondrial dysfunction causes skin aging, aging-associated hair loss,<sup>24</sup> and cutaneous pigmentary

changes.<sup>47</sup> These changes mimic changes related to aging in humans. The current study demonstrates that mitochondrial dysfunction in the whole animal induces morphologic and functional changes in SGs and MSGs. Changes in SG and MSG morphology and function share significant parallels with intrinsic and extrinsic age-related changes and altered SG activity and sebum composition in humans.<sup>19</sup> The gross and histopathologic changes in mtDNA depletor mice resemble skin pathologies reported in aging humans. These skin conditions include xerosis,<sup>48</sup> scaling, and the formation of yellowish umbilicated papules that resemble sebaceous hyperplasia with central puncta.<sup>49,50</sup> Furthermore, lesions similar to erythrosis interfollicularis colli, a common skin condition that occurs with chronic sun exposure on the neck of older people, resulting from sebaceous gland dilatation, were observed.<sup>51</sup> Additionally, dermal inflammation and matrix metalloprotease degradation of collagen was seen,

that has been reported previously in the skin of mtDNA depletor mouse model.<sup>24</sup>

Sebaceous glands are critical for the secretion of lipid-rich sebum that maintains tissue integrity, barrier functions, and skin hydration.<sup>1,52</sup> Age-associated reductions in sebum secretion have been reported in elderly individuals with increased incidence of skin infections<sup>53</sup> and development of age-related dry eye disease.<sup>54</sup> Inflammatory lesions noted in meibomian glands of mtDNA depletor mice are consistent with clinical signs of meibomian gland dysfunction seen in patients with changes in eyelid morphology, secretions, and gland dropout<sup>55</sup> associated with eyelid margin foaming, hyperemia, and changes in orifice position in relation to the mucocutaneous junction.<sup>56</sup> Interestingly, mtDNA depletor mice showed similar changes in lips and MSGs associated with accessory reproductive tissues, including the clitoris and prepuce. The current study is the first to describe that mitochondrial dysfunction is an important causative factor underlying the above conditions.

All SGs and MSGs of mtDNA depletor mice share a common feature of hyperplasia and destruction with surrounding mixed inflammatory reactions. To understand the role of peri-adnexal inflammation in the morphologic changes noted in SGs and MSGs, the localization and number of myeloid subsets, including mast cells, myeloperoxidase-positive neutrophils, and CD163<sup>+</sup> M2 macrophages were evaluated. These have been reported to infiltrate the surrounding dermis and epidermis, contributing to pathologic lesions in these anatomic regions of the skin.<sup>24</sup> Similar infiltration of peri-adnexal areas was seen with these inflammatory myeloid cells. Tissues enriched with large sebocytes, such as the mouse preputial gland, had a significant up-regulation of inflammatory mediator genes, including *Il1r1*, *Il6*, *TNF- $\alpha$* , and *COX2*. This suggested that morphologic changes are associated with chronic myeloid infiltrate and acute inflammatory mediator production. These observations are consistent with the similar mixed inflammatory reaction in the skin of the mtDNA depletor mouse model.<sup>24</sup> In addition, sebocytes are also directly capable of altering their sebum production/composition in response to various inflammatory stimuli.<sup>57–59</sup> Notably, superoxide dismutase 1 (Sod1) knockout mice show similar inflammatory responses and periglandular fibrosis of meibomian glands,<sup>60</sup> resulting in reduced meibomian gland secretions.

Evidence of glandular dysfunction manifesting as distension of SG and MSG with large lipid droplets (ORO), reduced skin surface lipid (ORO), and increased evidence of lipid oxidation (lipofuscin pigment accumulation) was noted. This was consistent with the gross, histologic, and inflammatory changes associated with the sebaceous and modified sebaceous glands. These findings support the gross signs of xerosis and scaliness noted in those animals and a standard feature reported in old-aged humans.<sup>19</sup> Furthermore, lipid accumulation in meibomian glands has been reported previously in old aged mice<sup>54</sup> and meibomian

glands of Sod1 knockout mice.<sup>60,61</sup> In addition, a significant up-regulation of lipogenesis-regulating genes (*Scd1*, *Prdm1*, and *Plin2*) has been noted in the MSG preputial gland. These genes play critical roles in SG/MSG development, sebocyte proliferation/homeostasis, and sebum production.

Sebocytes also express PPAR receptors with all three isoforms ( $\alpha$ ,  $\gamma$ , and  $\delta$ )<sup>16</sup> with varying effects on sebocyte proliferation and lipogenesis.<sup>18</sup> Previous studies showed increased human sebum production with PPAR  $\gamma$  and  $\delta$  agonists,<sup>62</sup> consistent with our results of up-regulation of peroxisome proliferator activator receptor delta (Ppard) and peroxisome proliferator activated receptor gamma (Pparg) in mtDNA depleted samples. Although PPAR $\alpha$  also plays a key role in mitochondrial  $\beta$ -oxidation and peroxisomal  $\beta$ -oxidation,<sup>63</sup> its ligands decrease SG lipid synthesis and perform significant reduction of acne lesions and sebaceous lipid synthesis,<sup>64</sup> similar to our observation of significantly lower expression of peroxisome proliferator activated receptor alpha (Ppara) in mtDNA depletor mice samples. Co-administration of androgens with ligands of PPARs augments the intracellular lipid accumulation in SGs of rat preputial gland,<sup>65</sup> as sebocytes express functional androgen receptors, and androgens may stimulate lipogenic differentiation by these cells. This can lead to increases in both sebum production and proinflammatory cytokine production by sebocytes,<sup>66</sup> emphasizing the sixfold increase of androgen receptor gene expression in mtDNA depletor mice compared with control.

Extensive accumulation of lipofuscin pigment during aging has been described.<sup>67</sup> The complex stress response resulting from mitochondrial dysfunction is proposed to induce cellular senescence.<sup>39,40</sup> The lipofuscin accumulates in the senescent cells with aging.<sup>32</sup> It represents the undegradable oxidized proteins (lipids and carbohydrates from cellular organelles that accumulate in lysosome) that get in skin photoaging.<sup>68,69</sup> Overall abnormal sebocyte lipofuscin accumulation confirms that mitochondrial dysfunction—induced inflammation accelerates aging-associated sebaceous gland damage and dysfunction.

Following the inflammatory and glandular-specific lesions indicative of SG and MSG dysfunction, sebocytes in these structures exhibited a high rate of cellular proliferation (Ki-67) within sebocytes at the basal layer of SGs. MSG maintenance of SGs depends on different progenitor cells at the periphery of the gland,<sup>33–35</sup> where there is an ongoing balance between proliferation and differentiation.<sup>10</sup> An imbalanced proliferation rate may accelerate stem cell exhaustion and decrease their regenerative capacity.<sup>70</sup> Furthermore, SG and MSG from mtDNA depletor mice exhibited a significant increase in stem cell markers. *Sox9*, *Lgr6*, *Lgr5*, *Gli1*, and *Gli2* have been detected at gene expression level by quantitative RT-PCR and protein expression with tissue immunohistochemical staining. *Sox9* has been reported to increase the proliferation colony-forming activity of human outer root sheath cells,<sup>71</sup> where skin SGs are considered an outgrowth of hair follicle outer

root sheath.<sup>6</sup> Sox9 overexpression enhanced proliferation, differentiation, lipogenesis, and PPAR $\gamma$  expression in sebocytes,<sup>41</sup> and has been expressed in basal cells of sebaceous neoplasms and implicated in its development.<sup>72</sup> *Lgr6* expression in sebocytes is noted in quiescent, long-lived stem cells<sup>42–45</sup> that have been reported to contribute to the regeneration of SG and interfollicular epidermis.<sup>46</sup> These observations suggest a regenerative process activated by chronic inflammation and oxidative damage as an attempt to reverse mitochondrial dysfunction—associated inflammation. This is similar to the current observation of increased *Lgr5* expression in mtDNA deleter mice. It has been reported that induction of *Lgr5* expression previously during embryogenesis and early development resulted in phenotypic and histologic changes of sparse fur coat and enlarged sebaceous glands, which were reversible on discontinued presentation of transgenic *Lgr5*.<sup>73</sup> Furthermore, increased *Gli1* and *Gli2* may be correlated with increased *Lgr5* expression. It has been reported previously that *Lgr5*-expressing skin showed an increase in the mRNA levels of Wnt5a and *Gli1*, the major effector of the Hedgehog pathway.<sup>73,74</sup>

The current studies revealed that mitochondrial dysfunction accounts for abnormal enlargement and lipogenesis associated with severe inflammation and destruction of SGs and MSGs in whole animals. There is a strong correlation between the mtDNA deleter mouse model and the human presentation of aging on SGs. The mtDNA deleter mouse can help define molecular mechanisms and identify genes and pathways underlying mitochondrial dysfunction—induced aging of SGs. This study can pave the way to develop novel strategies to treat aging-associated sebaceous gland dysfunction and identify drug targets to alleviate SG pathology and related skin disorders in humans.

## Acknowledgment

We thank Dr. Bhargavi Lakshmi for help with the bibliography.

## Author Contributions

K.K.S. conceived and conceptualized the study, and edited and revised the manuscript; N.S.A. designed the studies, performed and analyzed the experiments and histopathologic changes in tissues, conducted literature review, wrote the manuscript, and prepared figures and graphs; and J.B.F. supervised the study, conducted histopathologic analyses, and edited the manuscript.

## References

- Schneider MR, Paus R: Sebocytes, multifaceted epithelial cells: lipid production and holocrine secretion. *Int J Biochem Cell Biol* 2010, 42: 181–185
- Thody AJ, Shuster S: Control and function of sebaceous glands. *Physiol Rev* 1989, 69:383–416
- Smith KR, Thiboutot DM: Thematic review series: skin lipids: sebaceous gland lipids: friend or foe? *J Lipid Res* 2008, 49:271–281
- Feingold KR: The outer frontier: the importance of lipid metabolism in the skin. *J Lipid Res* 2009, 50:S417–S422
- Drake DR, Brogden KA, Dawson DV, Wertz PW: Thematic Review Series: skin lipids: antimicrobial lipids at the skin surface. *J Lipid Res* 2008, 49:4–11
- Thiboutot D: Regulation of human sebaceous glands. *J Invest Dermatol* 2004, 123:1–12
- Duke-Elder S: The anatomy of the visual system. *A Syst Ophthalmol* 1961, 2:363–382
- Wybar K: Wolff's anatomy of the eye and orbit. *Br J Ophthalmol* 1977, 61:302
- Reznik G, Reznik-Schüller H: Pathology of the clitoral and prepuccial glands in aging F344 rats. *Lab Anim Sci* 1980, 30:845–850
- Binczek E, Jenke B, Holz B, Günter RH, Thevis M, Stoffel W: Obesity resistance of the stearoyl-CoA desaturase-deficient (*scd1*-/-) mouse results from disruption of the epidermal lipid barrier and adaptive thermoregulation. *Biol Chem* 2007, 388:405–418
- Zouboulis CC, Degitz K: Androgen action on human skin - from basic research to clinical significance. *Exp Dermatol* 2004, 13(Suppl): 5–10
- Pochi PE, Strauss JS: Endocrinologic control of the development and activity of the human sebaceous gland. *J Invest Dermatol* 1974, 62: 191–201
- Hall DW, Van den Hoven WE, Noordzij-Kamerlings NJ, Jaitly KD: Hormonal control of hamster ear sebaceous gland lipogenesis. *Arch Dermatol Res* 1983, 275:1–7
- Kurokawa I, Danby FW, Ju Q, Wang X, Xiang LF, Xia L, Chen W, Nagy I, Picardo M, Suh DH, Ganceviciene R, Schagen S, Tsatsou F, Zouboulis CC: New developments in our understanding of acne pathogenesis and treatment. *Exp Dermatol* 2009, 18:821–832
- Makrantonaki E, Vogel K, Fimmel S, Oeff M, Seltmann H, Zouboulis CC: Interplay of IGF-I and 17 $\beta$ -estradiol at age-specific levels in human sebocytes and fibroblasts in vitro. *Exp Gerontol* 2008, 43:939–946
- Alesta T, Ganceviciene R, Fimmel S, Müller-Decker K, Zouboulis CC: Enzymes involved in the biosynthesis of leukotriene B4 and prostaglandin E2 are active in sebaceous glands. *J Mol Med* 2006, 84:75–87
- Chen W, Yang CC, Sheu HM, Seltmann H, Zouboulis CC: Expression of peroxisome proliferator-activated receptor and CCAAT/enhancer binding protein transcription factors in cultured human sebocytes. *J Invest Dermatol* 2003, 121:441–447
- Rosenfield RL, Deplewski D, Greene ME: Peroxisome proliferator-activated receptors and skin development. *Horm Res* 2000, 54: 269–274
- Zouboulis CC, Boschnakow A: Chronological ageing and photo-ageing of the human sebaceous gland. *Clin Exp Dermatol* 2001, 26: 600–607
- Sreedhar A, Aguilera-Aguirre L, Singh KK: Mitochondria in skin health, aging, and disease. *Cell Death Dis* 2020, 11:444
- Singh KK: Mitochondrial secrets of youthfulness. *Plast Reconstr Surg* 2021, 147:33S–37S
- Zouboulis CC, Yoshida GJ, Wu Y, Xia L, Schneider MR: Sebaceous gland: milestones of 30-year modelling research dedicated to the “brain of the skin.”. *Exp Dermatol* 2020, 29:1069–1079
- Lee HC, Wei YH: Mitochondria and aging. *Adv Exp Med Biol* 2012, 942:311–327
- Singh B, Schoeb TR, Bajpai P, Slominski A, Singh KK: Reversing wrinkled skin and hair loss in mice by restoring mitochondrial function. *Cell Death Dis* 2018, 9:735
- Lillie RD, Ashburn LL: Supersaturated solutions of fat stains in dilute isopropanol for demonstration of acute fatty degeneration not shown by Herxheimer's technique. *Arch Pathol* 1943, 36:432–440

26. Evangelou K, Gorgoulis VG: Sudan Black B, the specific histochemical stain for lipofuscin: a novel method to detect senescent cells. *Methods Mol Biol* 2017, 1534:111–119
27. Franceschi C, Bonafè M, Valensin S, Olivieri F, De luca M, Ottaviani E, De benedictis G: Inflamm-aging: an evolutionary perspective on immunosenescence. *Ann N Y Acad Sci* 2000, 908:244–254
28. Fulop T, Larbi A, Dupuis G, Le Page A, Frost EH, Cohen AA, Witkowski JM, Franceschi C: Immunosenescence and inflamm-aging as two sides of the same coin: friends or foes? *Front Immunol* 2018, 8:1960
29. Salvioli S, Capri M, Valensin S, Tieri P, Monti D, Ottaviani E, Franceschi C: Inflamm-aging, cytokines and aging: state of the art, new hypotheses on the role of mitochondria and new perspectives from systems biology. *Curr Pharm Des* 2006, 12:3161–3171
30. Nagy I, Pivarsci A, Kis K, Koreck A, Bodai L, McDowell A, Seltmann H, Patrick S, Zouboulis CC, Kemény L: Propionibacterium acnes and lipopolysaccharide induce the expression of antimicrobial peptides and proinflammatory cytokines/chemokines in human sebocytes. *Microbes Infect* 2006, 8:2195–2205
31. Abu Bakar MH, Hassan W, Sarmidi M, Yaakob H: Mitochondrial dysfunction enhances lipolysis and intracellular lipid accumulation in 3T3-L1 adipocytes. *Int J Pharma Med Biol Sci* 2015, 4:65–69
32. Georgakopoulou EA, Tsimaratou K, Evangelou K, Fernandez Marcos PJ, Zoumpourlis V, Trougakos IP, Kletsas D, Bartek J, Serrano M, Gorgoulis VG: Specific lipofuscin staining as a novel biomarker to detect replicative and stress-induced senescence: a method applicable in cryo-preserved and archival tissues. *Aging (Albany NY)* 2013, 5:37–50
33. Ghazizadeh S, Taichman LB: Multiple classes of stem cells in cutaneous epithelium: a lineage analysis of adult mouse skin. *EMBO J* 2001, 20:1215–1222
34. Horsley V, O'Carroll D, Tooze R, Ohinata Y, Saitou M, Obukhanych T, Nussenzweig M, Tarakhovsky A, Fuchs E: Blimp1 defines a progenitor population that governs cellular input to the sebaceous gland. *Cell* 2006, 126:597–609
35. Jensen KB, Collins CA, Nascimento E, Tan DW, Frye M, Itami S, Watt FM: Lrig1 expression defines a distinct multipotent stem cell population in mammalian epidermis. *Cell Stem Cell* 2009, 4:427–439
36. Conboy IM, Conboy MJ, Smythe GM, Rando TA: Notch-mediated restoration of regenerative potential to aged muscle. *Science* 2003, 302:1575–1577
37. Rossi DJ, Bryder D, Zahn JM, Ahlenius H, Sonu R, Wagers AJ, Weissman IL: Cell intrinsic alterations underlie hematopoietic stem cell aging. *Proc Natl Acad Sci U S A* 2005, 102:9194
38. Molofsky AV, Slutsky SG, Joseph NM, He S, Pardoll R, Krishnamurthy J, Sharpless NE, Morrison SJ: Increasing p16INK4a expression decreases forebrain progenitors and neurogenesis during ageing. *Nature* 2006, 443:448–452
39. Braig M, Schmitt CA: Oncogene-induced senescence: putting the brakes on tumor development. *Cancer Res* 2006, 66:2881–2884
40. Campisi J, d'Adda di Fagagna F: Cellular senescence: when bad things happen to good cells. *Nat Rev Mol Cell Biol* 2007, 8:729–740
41. Shi G, Wang TT, Quan JH, Li SJ, Zhang MF, Liao PY, Fan YM: Sox9 facilitates proliferation, differentiation and lipogenesis in primary cultured human sebocytes. *J Dermatol Sci* 2017, 85:44–50
42. Gong X, Carmon KS, Lin Q, Thomas A, Yi J, Liu Q: LGR6 is a high affinity receptor of R-Spondins and potentially functions as a tumor suppressor. *PLoS One* 2012, 7:e37137
43. Page MEE, Lombard P, Ng F, Göttgens B, Jensen KBB: The epidermis comprises autonomous compartments maintained by distinct stem cell populations. *Cell Stem Cell* 2013, 13:471–482
44. Liao XH, Nguyen H: Epidermal expression of Lgr6 is dependent on nerve endings and Schwann cells. *Exp Dermatol* 2014, 23:195–198
45. Kretschmar K, Weber C, Driskell RR, Calonje E, Watt FM: Compartmentalized epidermal activation of  $\beta$ -catenin differentially affects lineage reprogramming and underlies tumor heterogeneity. *Cell Rep* 2016, 14:269–281
46. Snippet HJ, Haegebarth A, Kasper M, Jaks V, van Es JH, Barker N, van de Wetering M, van den Born M, Begthel H, Vries RG, Stange DE, Toftgård R, Clevers H: Lgr6 marks stem cells in the hair follicle that generate all cell lineages of the skin. *Science* 2010, 327:1385–1389
47. Villavicencio KM, Ahmed N, Harris ML, Singh KK: Mitochondrial DNA-deleter mouse as a model to study human pigmentary skin disorders. *Pigment Cell Melanoma Res* 2021, 34:179–187
48. Angelides AP: Winter ailments of the old. *J Gerontol* 1947, 2:85–86
49. Belinchón I, Aguilar A, Tardío J, Gallego MA: Areolar sebaceous hyperplasia: a case report. *Cutis* 1996, 58:63–64
50. Boonchai W, Leenutaphong V: Familial presenile sebaceous gland hyperplasia. *J Am Acad Dermatol* 1997, 36:120–122
51. Wollina U: Erythrosis interfollicularis colli and cutis rhomboidalis nuchae: two sides of a coin. *Acta Dermatovenerol Alp Pannonica Adriat* 2019, 28:53–55
52. Niemann C: Differentiation of the sebaceous gland. *Dermatoendocrinol* 2009, 1:64–67
53. Jacobsen E, Billings JK, Frantz RA, Kinney CK, Stewart ME, Downing DT: Age-related changes in sebaceous wax ester secretion rates in men and women. *J Invest Dermatol* 1985, 85:483–485
54. Nien CJ, Paugh JR, Massei S, Wahlert AJ, Kao WW, Jester JV: Age-related changes in the meibomian gland. *Exp Eye Res* 2009, 89:1021–1027
55. Tomlinson A, Bron AJ, Korb DR, Amano S, Paugh JR, Pearce EI, Yee R, Yokoi N, Arita R, Dogru M: The international workshop on meibomian gland dysfunction: report of the diagnosis subcommittee. *Invest Ophthalmol Vis Sci* 2011, 52:2006–2049
56. Chhadva P, Goldhardt R, Galor A: Meibomian gland disease: the role of gland dysfunction in dry eye disease. *Ophthalmology* 2017, 124:S20–S26
57. Dobrosi N, Tóth BI, Nagy G, Dózsa A, Géczy T, Nagy L, Zouboulis CC, Paus R, Kovács L, Bíró T: Endocannabinoids enhance lipid synthesis and apoptosis of human sebocytes via cannabinoid receptor-2-mediated signaling. *FASEB J* 2008, 22:3685–3695
58. Géczy T, Oláh A, Tóth BI, Czifra G, Szöllösi AG, Szabó T, Zouboulis CC, Paus R, Bíró T: Protein kinase C isoforms have differential roles in the regulation of human sebocyte biology. *J Invest Dermatol* 2012, 132:1988–1997
59. Töröcsik D, Kovács D, Camera E, Lovászi M, Cseri K, Nagy GG, Molinaro R, Rühl R, Tax G, Szabó K, Picardo M, Kemény L, Zouboulis CC, Remenyik É: Leptin promotes a proinflammatory lipid profile and induces inflammatory pathways in human SZ95 sebocytes. *Br J Dermatol* 2014, 171:1326–1335
60. Ibrahim OM, Dogru M, Matsumoto Y, Igarashi A, Kojima T, Wakamatsu TH, Inaba T, Shimizu T, Shimazaki J, Tsubota K: Oxidative stress induced age dependent meibomian gland dysfunction in Cu, Zn-superoxide dismutase-1 (Sod1) knockout mice. *PLoS One* 2014, 9:e99328
61. Sullivan BD, Evans JE, Dana MR, Sullivan DA: Influence of aging on the polar and neutral lipid profiles in human meibomian gland secretions. *Arch Ophthalmol* 2006, 124:1286–1292
62. Trivedi NR, Cong Z, Nelson AM, Albert AJ, Rosamilia LL, Sivarajah S, Gilliland KL, Liu W, Mauger DT, Gabbay RA, Thiboutot DM: Peroxisome proliferator-activated receptors increase human sebum production. *J Invest Dermatol* 2006, 126:2002–2009
63. Motojima K, Passilly P, Peters JM, Gonzalez FJ, Latruffe N: Expression of putative fatty acid transporter genes are regulated by peroxisome proliferator-activated receptor  $\alpha$  and  $\gamma$  activators in a tissue- and inducer-specific manner. *J Biol Chem* 1998, 273:16710–16714
64. Zouboulis CC, Seltmann H, Alestas T: Zileuton prevents the activation of the leukotriene pathway and reduces sebaceous lipogenesis. *Exp Dermatol* 2010, 19:148–150
65. Rosenfield RL, Kentsis A, Deplewski D, Ciletti N: Rat preputial sebocyte differentiation involves peroxisome proliferator-activated receptors. *J Invest Dermatol* 1999, 112:226–232
66. Lee WJ, Jung HD, Chi SG, Kim BS, Lee SJ, Kim DW, Kim MK, Kim JC: Effect of dihydrotestosterone on the upregulation of

- inflammatory cytokines in cultured sebocytes. *Arch Dermatol Res* 2010, 302:429–433
67. Skoczyńska A, Budzisz E, Trznadel-Grodzka E, Rotsztein H: Melanin and lipofuscin as hallmarks of skin aging. *Postepy Dermatol Alergol* 2017, 34:97–103
  68. Sander CS, Chang H, Salzmann S, Müller CS, Ekanayake-Mudiyanselage S, Elsner P, Thiele JJ: Photoaging is associated with protein oxidation in human skin in vivo. *J Invest Dermatol* 2002, 118: 618–625
  69. Yaar M, Gilchrist BA: Photoageing: mechanism, prevention and therapy. *Br J Dermatol* 2007, 157:874–887
  70. Ahlqvist KJ, Suomalainen A, Hämäläinen RH: Stem cells, mitochondria and aging. *Biochim Biophys Acta* 2015, 1847: 1380–1386
  71. Shi G, Sohn K-C, Kim S-Y, Ryu E-K, Park Y-S, Lee Y, Seo Y-J, Lee J-H, Kim CD: Sox9 increases the proliferation and colony-forming activity of outer root sheath cells cultured in vitro. *Ann Dermatol* 2011, 23:138–143
  72. Qiu W, Lei M, Li J, Wang N, Lian X: Activated hair follicle stem cells and Wnt/ $\beta$ -catenin signaling involve in pathogenesis of sebaceous neoplasms. *Int J Med Sci* 2014, 11:1022–1028
  73. Norum JH, Bergström Å, Andersson AB, Kuiper RV, Hoelzl MA, Sørli T, Toftgård R: A conditional transgenic mouse line for targeted expression of the stem cell marker LGR5. *Dev Biol Dev Biol* 2015, 404:35–48
  74. Niemann C, Uden AB, Lyle S, Zouboulis CC, Toftgård R, Watt FM: Indian hedgehog and  $\beta$ -catenin signaling: role in the sebaceous lineage of normal and neoplastic mammalian epidermis. *Proc Natl Acad Sci U S A* 2003, 100:11873–11880